

Supplement of Atmos. Meas. Tech., 9, 2735–2752, 2016  
<http://www.atmos-meas-tech.net/9/2735/2016/>  
doi:10.5194/amt-9-2735-2016-supplement  
© Author(s) 2016. CC Attribution 3.0 License.



Atmospheric  
Measurement  
Techniques

Open Access



*Supplement of*

## **A high-resolution time-of-flight chemical ionization mass spectrometer utilizing hydronium ions ( $\text{H}_3\text{O}^+$ ToF-CIMS) for measurements of volatile organic compounds in the atmosphere**

**Bin Yuan et al.**

*Correspondence to:* Bin Yuan (bin.yuan@noaa.gov)

The copyright of individual parts of the supplement might differ from the CC-BY 3.0 licence.

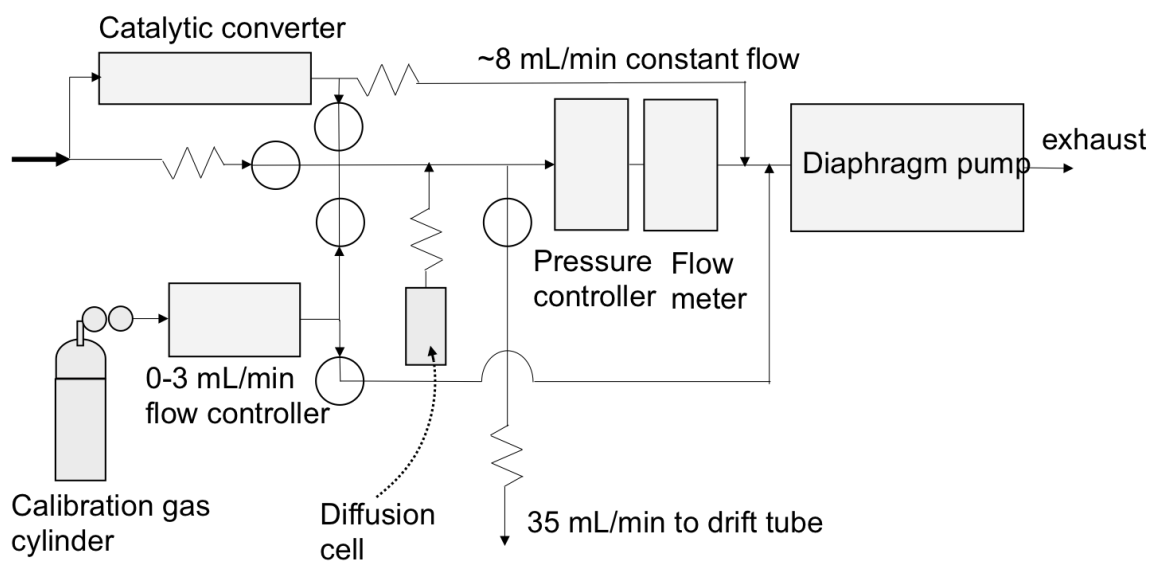
## 15 **Mass resolving power and separation of isobaric masses**

16 The mass resolving power ( $m/\Delta m$ ) was derived from the observed linear  
17 relationship between the full-width half maximum (FWHM) of several isolated mass  
18 peaks and their  $m/z$  using Tofware (Stark et al., 2015). The typical  $m/\Delta m$  for the  $\text{H}_3\text{O}^+$   
19 ToF-CIMS during the SONGNEX campaign is shown in Figure S2. The  $m/\Delta m$  in the  
20 range of  $m/z$  30 - 200 (where most VOCs were detected), are 3900-5900 with higher  
21 resolution for heavier masses. These mass resolutions are sufficient to separate many  
22 isobaric ions. Figure S3 shows the separation of C8 aromatics ( $\text{C}_8\text{H}_{10}\text{H}^+$ ,  $m/z$  107.086)  
23 from benzaldehyde ( $\text{C}_7\text{H}_6\text{OH}^+$ ,  $m/z$  107.049) for  $m/z$  107 during a flight leg (18:15-18:45  
24 UTC) over the Permian Basin in Texas, US. The two mass spectra in A and B are 30 s  
25 averages centered around 18:25:00 and 18:35:10, respectively. The two time windows  
26 had either benzaldehyde or C8 aromatics as the higher peak between the two. The time  
27 series of benzaldehyde and C8 aromatics determined from the mass spectral fits for this  
28 30-min period correlated well with acetone ( $R=0.87$ ) and benzene ( $R=0.94$ ), respectively.  
29 This is consistent with the expectation that benzaldehyde was mainly from secondary  
30 formation and C8 aromatics were dominated by primary emissions from oil and gas  
31 activities. The signals at  $m/z$  107 are usually assigned to C8 aromatics in PTR-QMS  
32 studies (de Gouw and Warneke, 2007). Although the possible interference from  
33 benzaldehyde to C8 aromatics has been known, it usually constitutes a small fraction of  
34 the total signal at nominal mass 107 (Warneke et al., 2003). The example shown in  
35 Figure S3 indicates that benzaldehyde, in some environments, can contribute significantly  
36 to signals at nominal mass 107.

37 Based on results in previous studies (Graus et al., 2010; Stark et al., 2015), the mass  
38 resolving power of the ToF analyzer presented in this study can separate many of the  
39 isobaric masses in the mass range of  $m/z < 200$  by utilizing the high-resolution peak fitting  
40 algorithms. The separation of isobaric ions has several advantages over the nominal mass  
41 data of PTR-QMS: (1) reduce chemical interferences, e.g. the interference of  
42 benzaldehyde to C8 aromatics at nominal  $m/z$  107 as shown above; (2) decrease  
43 background signals for several compounds of interest, e.g. for methanol (Müller et al.,  
44 2014) and acetaldehyde, the instrument backgrounds of which have interferences from  
45  $\text{O}_2\text{H}^+$  and  $\text{CO}_2\text{H}^+$  at the same nominal masses, respectively; (3) increase the number of

46 species that can be measured. In general, 10-20 compounds are usually measurable by the  
47 PTR-QMS explicitly without significant interference depending on the origin of the air  
48 masses (de Gouw and Warneke, 2007). During the SONGNEX campaign, a total of 1055  
49 peaks between  $m/z$  12 and  $m/z$  181 were identified and assigned to signals in the mass  
50 spectra of  $H_3O^+$  ToF-CIMS. Not all of these mass signals can be used for VOC  
51 quantification. Many masses (1) are associated with large errors from high-resolution  
52 peak fittings as the result of a much larger peak nearby and/or poor separation from  
53 another peak; or (2) have no significant enhancement over instrument background. Over  
54 260 masses had periods (at least 1 min) with signal to background ratios larger than three  
55 during the flight over the Permian Basin on April 23, 2015. Although not all of these  
56 masses are attributable to specific compounds, chemical formulas of the masses give  
57 more detailed information on the chemical composition than just the nominal  $m/z$ .  
58 Detailed interpretation of the mass spectra in various air masses during the SONGNEX  
59 campaign will be presented in a separate publication (Koss et al., in prep).  
60

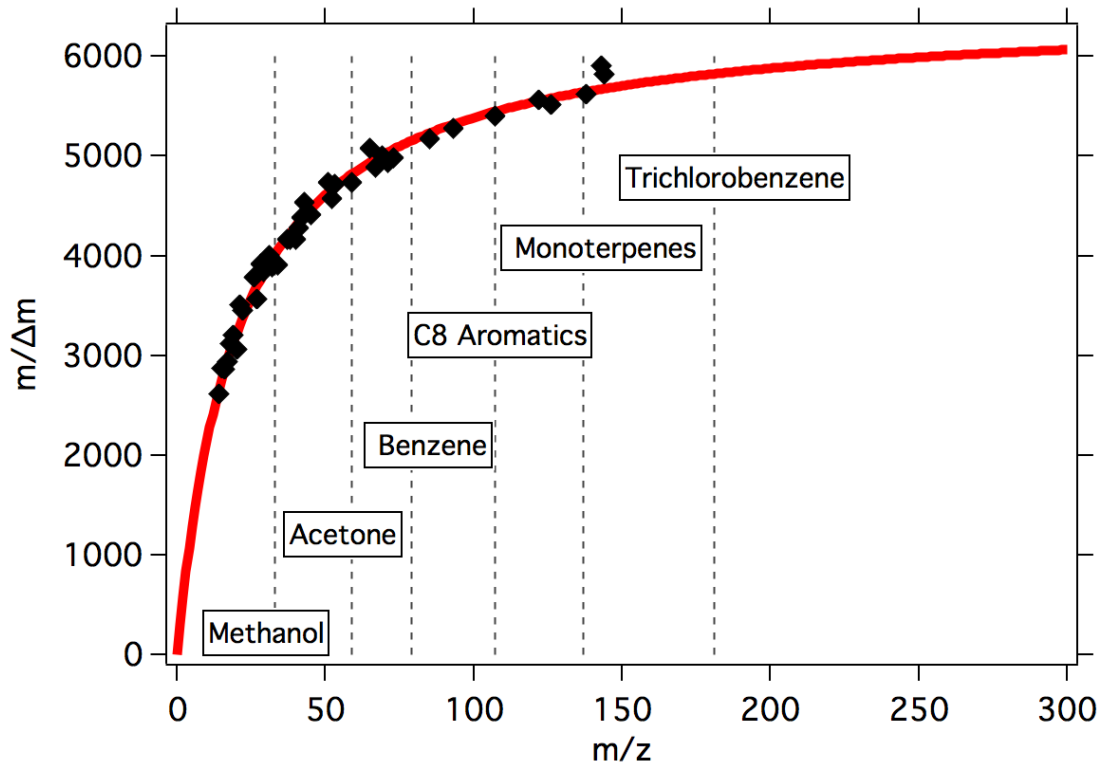
61 **Figures**



62

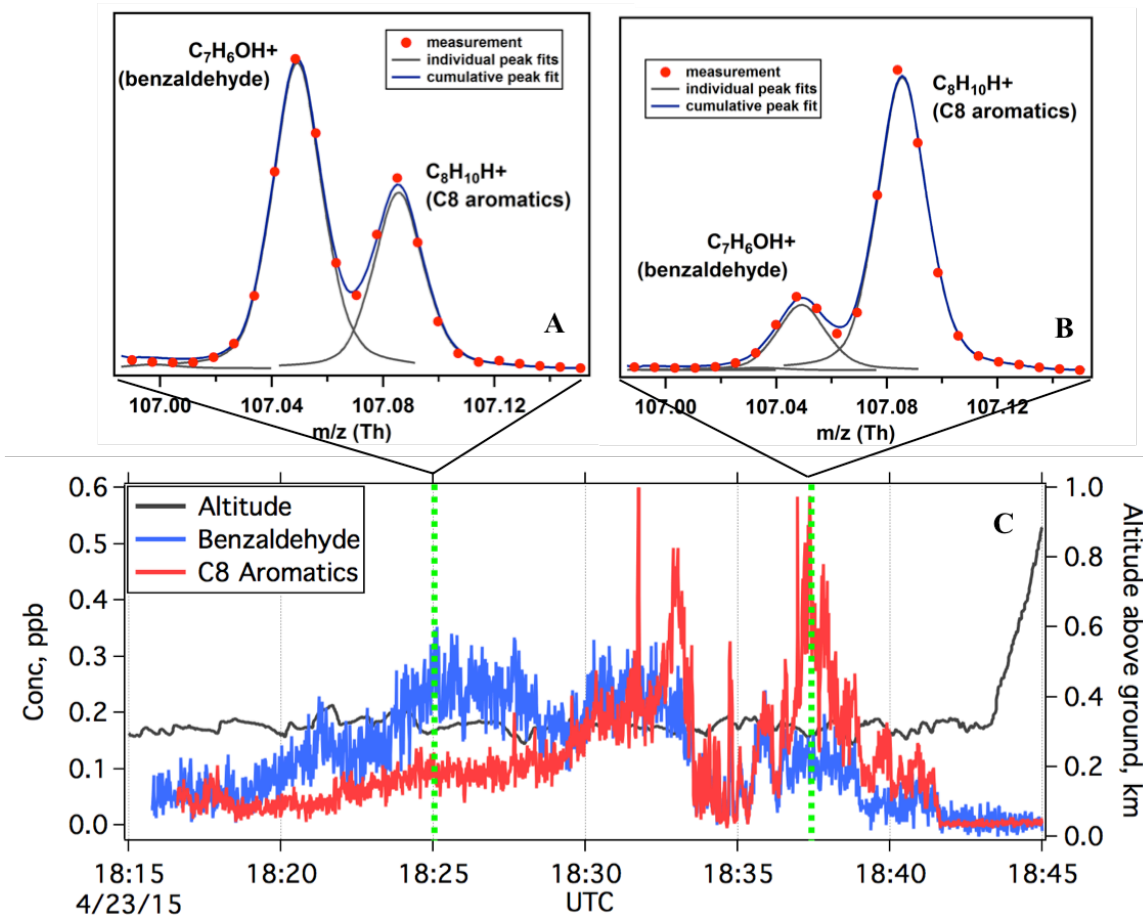
63 Figure S1. Inlet diagram used during the SONGNEX campaign

64



65

66 Figure S2. Mass resolution ( $m/\Delta m$ ) of the ToF analyzer from measured data in the flight  
 67 on April 13, 2015. The black markers are the calculated  $m/\Delta m$  from isolated  $m/z$  peaks.  
 68 The red curve indicates the fitted line in the range of  $m/z$  0-300. Vertical dashed lines  
 69 indicate the positions of several VOC species (methanol, acetone, benzene, C8 aromatics,  
 70 monoterpenes and trichlorobenzenes).

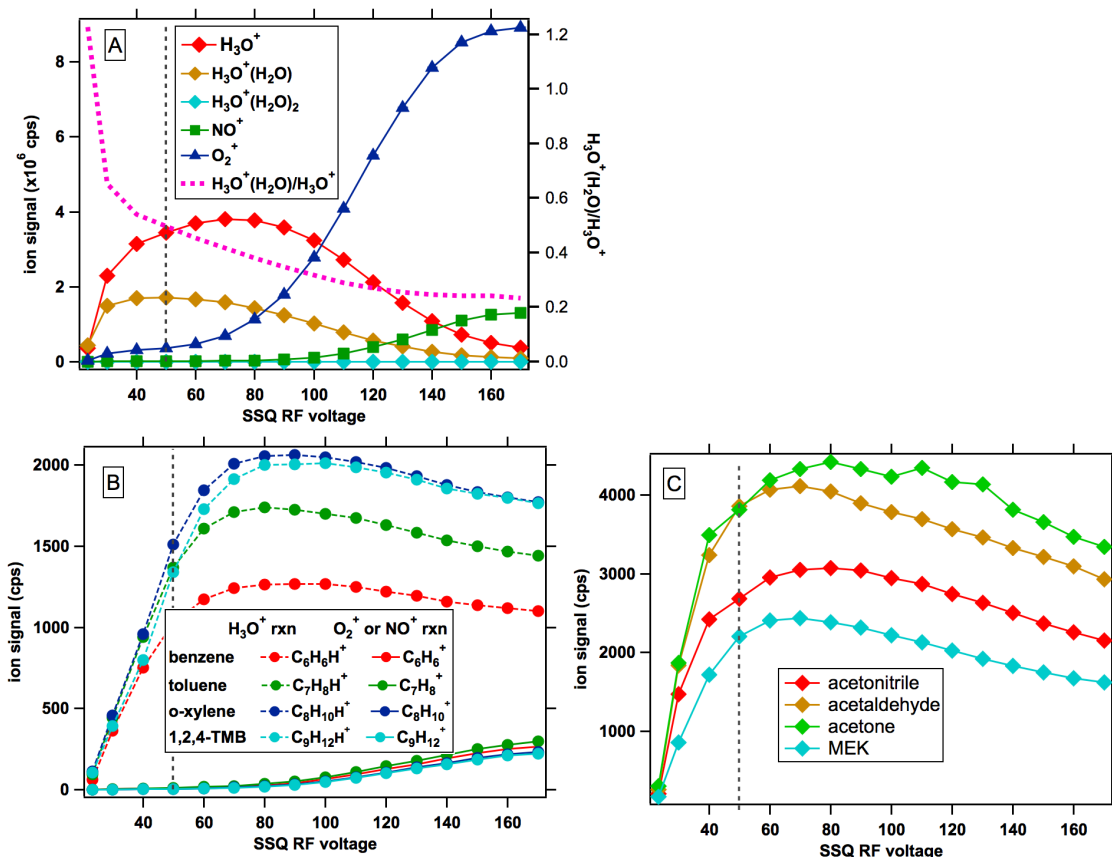


71

72 Figure S3. Separation of benzaldehyde and C8 aromatics from the nominal mass at  $m/z$   
 73 107 in a period (18:15-18:45 UTC) during the flight over the Permian Basin on April 23,  
 74 2015. (A and B) HR peak fittings of mass spectra at  $m/z$  107 at 18:25 and 18:37,  
 75 respectively. (C) Time series of benzaldehyde and C8 aromatics during the period. Flight  
 76 altitude of the NOAA WP-3D aircraft is included in C.

77

78

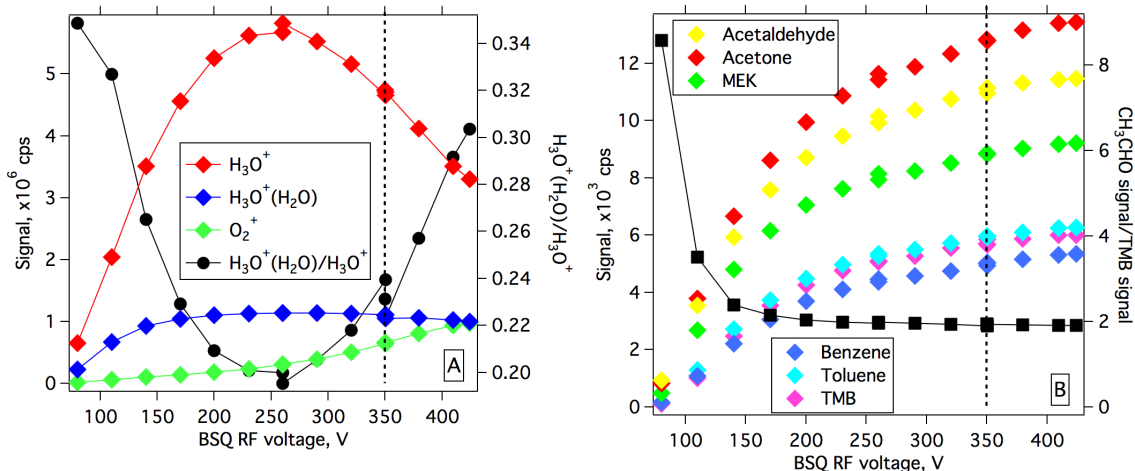


79

80 Figure S4. Signals of the reagent ions and VOC product ions as a function of the RF  
 81 amplitudes in the SSQ. (A) Signals of  $\text{H}_3\text{O}^+$ ,  $\text{H}_3\text{O}^+(\text{H}_2\text{O})$ ,  $\text{H}_3\text{O}^+(\text{H}_2\text{O})_2$ ,  $\text{NO}^+$  and  $\text{O}_2^+$  as a  
 82 function of RF amplitudes of the SSQ.  $\text{H}_3\text{O}^+(\text{H}_2\text{O})/\text{H}_3\text{O}^+$  ratios as a function of RF  
 83 amplitudes are also shown in A. (B) Product ions from proton transfer and charge transfer  
 84 reactions of aromatics (benzene, toluene, o-xylene and 1,2,4-trimethylbenzene) as a  
 85 function of RF amplitudes of the SSQ. (C) Product ions of acetonitrile, acetaldehyde,  
 86 acetone and MEK as a function of RF amplitudes of the SSQ. The vertical dashed lines  
 87 indicate the RF amplitudes of the SSQ (50 V) used during the SONGNEX campaign.

88

89



90

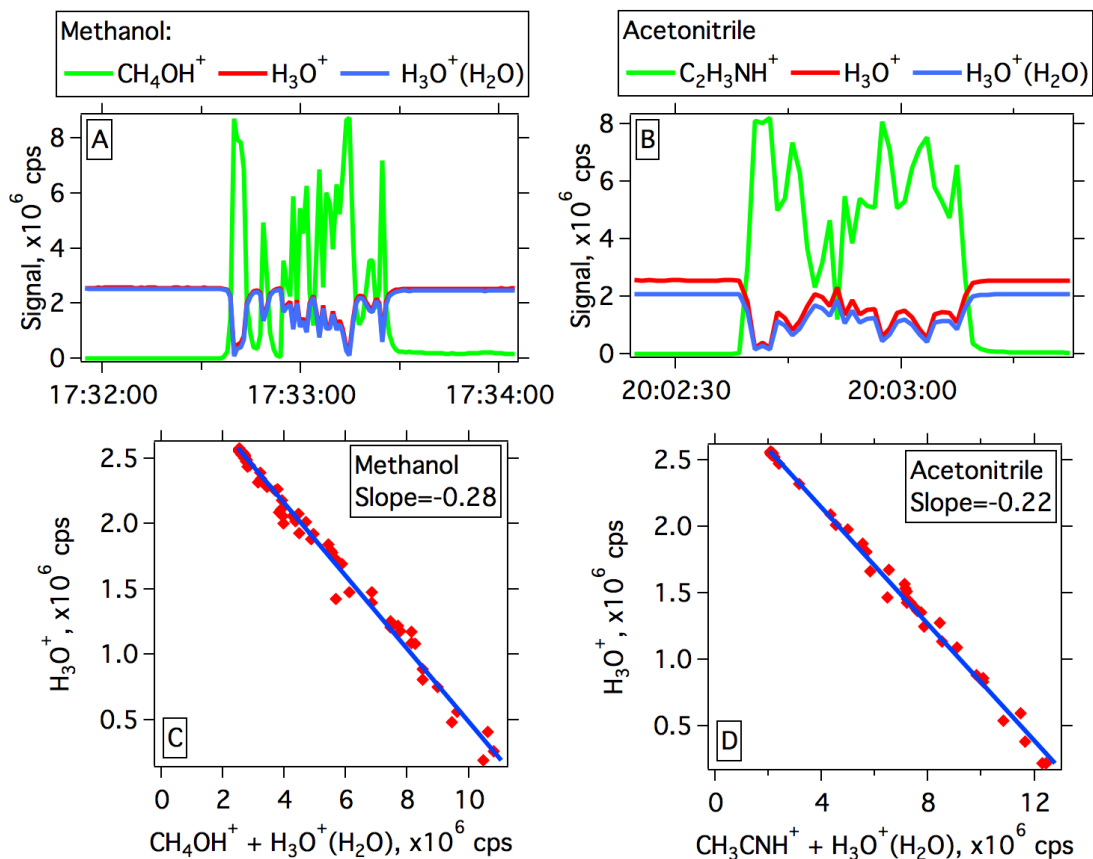
91 Figure S5. (A) Signals of H<sub>3</sub>O<sup>+</sup>, H<sub>3</sub>O<sup>+</sup>(H<sub>2</sub>O) and O<sub>2</sub><sup>+</sup> as a function of RF amplitudes of the  
 92 BSQ. H<sub>3</sub>O<sup>+</sup>(H<sub>2</sub>O)/ H<sub>3</sub>O<sup>+</sup> ratios as a function of RF amplitudes of the BSQ are also shown  
 93 in A. (B) Product ions of several VOCs (acetaldehyde, acetone, MEK, benzene, toluene  
 94 and 1,2,4-trimethylbenzene) as a function of RF amplitudes of the BSQ. The ratios of  
 95 acetaldehyde signals to 1,2,4-trimethylbenzene signals as a function of RF amplitudes of  
 96 the BSQ are included. The vertical dashed lines indicate the RF amplitudes of BSQ (350  
 97 V) used during the SONGNEX campaign.

98

99

100





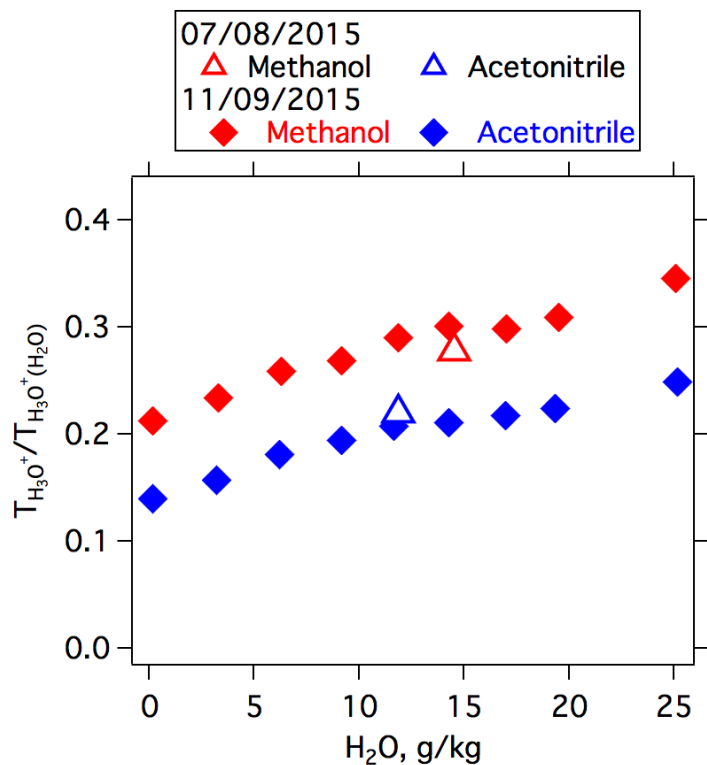
101

102 Figure S6. (A and B) Time series of the signals of the reagent ions and protonated  
 103 product ions when large amounts of methanol (A) and acetonitrile (B) were introduced  
 104 into the instrument. (C and D) Scatterplots of H<sub>3</sub>O<sup>+</sup> ions versus the sums of protonated  
 105 product ions and H<sub>3</sub>O<sup>+</sup>(H<sub>2</sub>O) ions from methanol and acetonitrile experiments shown in  
 106 (A) and (B), respectively. The blue lines are linear fits to the data points. The slopes of  
 107 linear fits represent the ratios of transmission efficiency between H<sub>3</sub>O<sup>+</sup> and H<sub>3</sub>O<sup>+</sup>(H<sub>2</sub>O)  
 108 ( $T_{H_3O^+}/T_{H_3O^+(H_2O)}$ ).

109

110

111

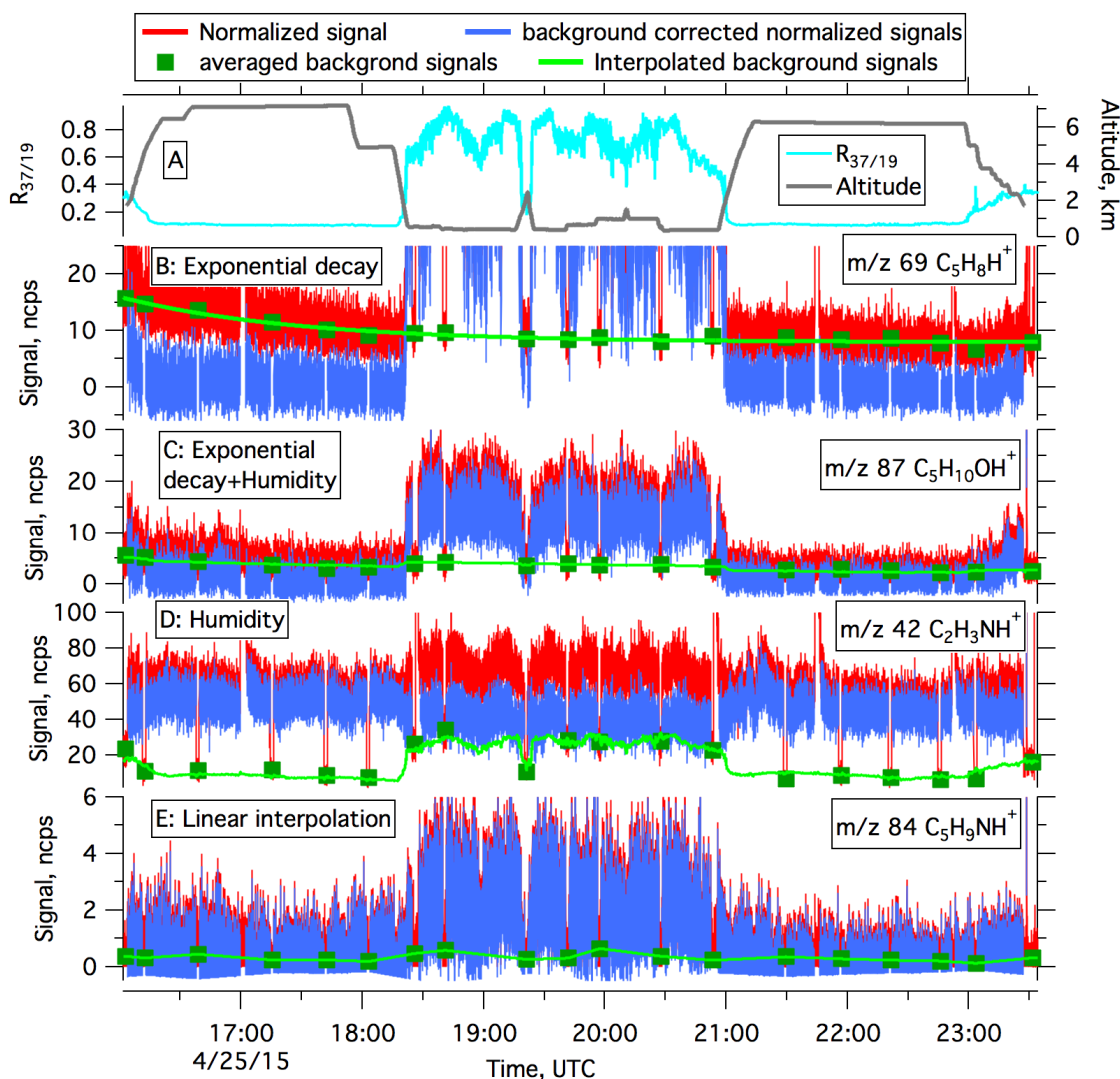


112

113 Figure S7. The determined ratios of transmission efficiency between  $H_3O^+$  and  
 114  $H_3O^+(H_2O)$  ( $T_{H_3O^+}/T_{H_3O^+(H_2O)}$ ) as a function of water vapor mixing ratios of the sampled  
 115 air from the experiments of introducing large concentrations of methanol and acetonitrile,  
 116 respectively (Figure S4). Experiments were performed on July 8 and November 9, with  
 117 measurements at different humidity levels on November 9, 2015. Consistent estimates  
 118 were derived from the experiments in July and November.

119





129

130 Figure S9. Background correction for several ions for the flight on April 25, 2015 over  
 131 the Haynesville during SONGNEX. (A) Time series of  $\text{H}_3\text{O}^+(\text{H}_2\text{O})/\text{H}_3\text{O}^+$  ( $R_{37/19}$ ) and  
 132 aircraft altitude during the flight. (B-E) Time series of the normalized signals, averaged  
 133 background signals, interpolated background signals and the background corrected  
 134 signals for the ions of  $\text{C}_5\text{H}_8\text{H}^+$  ( $m/z$  69.070),  $\text{C}_5\text{H}_{10}\text{OH}^+$  ( $m/z$  87.080),  $\text{C}_2\text{H}_3\text{NH}^+$  ( $m/z$   
 135 42.034) and  $\text{C}_5\text{H}_9\text{NH}^+$  ( $m/z$  84.081) to illustrate background correction algorithms with  
 136 exponential decay, exponential decay+humidity, humidity dependence and linear  
 137 interpolation, respectively.

138

139

140 **References:**

- 141 de Gouw, J., and Warneke, C.: Measurements of volatile organic compounds in the  
142 earth's atmosphere using proton-transfer-reaction mass spectrometry, *Mass*  
143 *Spectrometry Reviews*, 26, 223-257, 2007.
- 144 Graus, M., Muller, M., and Hansel, A.: High Resolution PTR-TOF: Quantification and  
145 Formula Confirmation of VOC in Real Time, *Journal of the American Society for*  
146 *Mass Spectrometry*, 21, 1037-1044, DOI 10.1016/j.jasms.2010.02.006, 2010.
- 147 Müller, M., Mikoviny, T., Feil, S., Haidacher, S., Hanel, G., Hartungen, E., Jordan, A.,  
148 Märk, L., Mutschlechner, P., Schotchkowsky, R., Sulzer, P., Crawford, J. H., and  
149 Wisthaler, A.: A compact PTR-ToF-MS instrument for airborne measurements of  
150 volatile organic compounds at high spatiotemporal resolution, *Atmos. Meas.*  
151 *Tech.*, 7, 3763-3772, 10.5194/amt-7-3763-2014, 2014.
- 152 Stark, H., Yatayelli, R. L. N., Thompson, S. L., Kimmel, J. R., Cubison, M. J., Chhabra,  
153 P. S., Canagaratna, M. R., Jayne, J. T., Worsnop, D. R., and Jimenez, J. L.:  
154 Methods to extract molecular and bulk chemical information from series of  
155 complex mass spectra with limited mass resolution, *International Journal of Mass*  
156 *Spectrometry*, 389, 26-38, 10.1016/j.ijms.2015.08.011, 2015.
- 157 Warneke, C., De Gouw, J. A., Kuster, W. C., Goldan, P. D., and Fall, R.: Validation of  
158 atmospheric VOC measurements by proton-transfer-reaction mass spectrometry  
159 using a gas-chromatographic pre-separation method, *Environmental Science &*  
160 *Technology*, 37, 2494-2501, 10.1021/es026266i, 2003.
- 161